ChemPubSoc Europe
DOI: 10.1002/cmdc.201500422
CHEMMEDCHEM Full Papers

SPECIAL ISSUE

Nature-Inspired Multifunctional Ligands: Focusing on Amyloid-Based Molecular Mechanisms of Alzheimer's Disease

Elena Simoni,[a] Melania M. Serafini,[b] Manuela Bartolini,[a] Roberta Caporaso,[a] Antonella Pinto,[b] Daniela Necchi,[b] Jessica Fiori,[a] Vincenza Andrisano,[c] Anna Minarini,[a] Cristina Lanni,*[b] and Michela Rosini*[a]

The amyloidogenic pathway is a prominent feature of Alzheimer's disease (AD). However, growing evidence suggests that a linear disease model based on β-amyloid peptide (Aβ) alone is not likely to be realistic, which therefore calls for further investigations on the other actors involved in the play. The prooxidant environment induced by Aβ in AD pathology is well established, and a correlation among Aβ, oxidative stress, and conformational changes in p53 has been suggested. In this study, we applied a multifunctional approach to identify allyl thioesters of variously substituted *trans*-cinnamic acids for which the pharmacological profile was strategically tuned by hydroxy substituents on the aromatic moiety. Indeed, only catechol derivative **3** [(*S*)-allyl (*E*)-3-(3,4-dihydroxyphenyl)prop-2-enethioate] inhibited Aβ fibrilization. Conversely, albeit to different extents, all compounds were able to decrease the formation of reactive oxygen species in SH-SY5Y neuroblastoma cells and to prevent alterations in the conformation of p53 and its activity mediated by soluble sub-lethal concentrations of Aβ. This may support an involvement of oxidative stress in Aβ function, with p53 emerging as a potential mediator of their functional interplay.

Introduction

Alzheimer's disease (AD) is a progressive neurodegenerative disorder, with a complex interplay of genetic and biochemical factors contributing to pathological decline. Progression of the disease involves misfolding and aggregation of β-amyloid peptide (Aβ) from soluble nontoxic monomers into insoluble fibrils. The most toxic form of Aβ is believed to be soluble oligomers, which are potent mediators of synaptotoxicity.[1] In AD drug development, programs based on the Aβ cascade hypothesis have dominated research for the past 20 years and still play a major role in pharmaceutical product pipelines. However, Aβ-centric approaches have not yet resulted in clinically effective drugs. This has raised a degree of skepticism, which has in turn led to a review of the science underpinning the Aβ model.[2] Besides the consolidated evidence that Aβ might trigger the disease process, intertwined correlations between Aβ and the other main players of the disease have been identified.[3] This has prompted researchers to develop multifunctional anti-amyloid agents[4] that, by acting simultaneously on several AD targets instead of the amyloidogenic pathway alone, are intended to trigger a synergistic response with superior efficacy and safety profile.[5] Further, we think that molecules endowed with a multifaceted pharmacology have great potential in exploring the Aβ partnership with other crucial AD features. A deeper comprehension of amyloid-based disease mechanisms might offer the chance for the repositioning of Aβ in the disease network, which would be of help in bridging the gap between basic and translational research. In particular, the etiopathogenic loop generated by Aβ and oxidative stress offers a new key for reading the causative role of Aβ.[6] Oxidative stress is known to trigger the amyloidogenic pathway and to promote Aβ toxicity.[7] On the other hand, several lines of evidence indicate that Aβ exacerbates oxidative stress, with other cellular pathways emerging as determining mediators of this vicious cycle.[8] In this respect, regulation of the conformation and function of p53 may represent a crucial feature of this puzzling scenario.

p53 is a tumor-suppressor protein primarily involved in cancer biology. However, recent observations have showed that p53 may also play a central role in aging and in neurodegenerative disorders.[9] Conformational changes and functional alterations of p53 have been found in patients with AD.[10] Unfolded p53 is not able to exert its pro-apoptotic activity in AD

[a] Dr. E. Simoni, Prof. Dr. M. Bartolini, R. Caporaso, Dr. J. Fiori, Prof. Dr. A. Minarini, Prof. Dr. M. Rosini
Department of Pharmacy and Biotechnology
Alma Mater Studiorum, University of Bologna
Via Belmeloro 6, 40126 Bologna (Italy)
E-mail: michela.rosini@unibo.it

[b] M. M. Serafini, A. Pinto, Dr. D. Necchi, Dr. C. Lanni
Department of Drug Sciences (Pharmacology Section)
University of Pavia, V.le Taramelli 14, 27100 Pavia (Italy)
E-mail: cristina.lanni@unipv.it

[c] Prof. Dr. V. Andrisano
Department for Life Quality Studies
Alma Mater Studiorum, University of Bologna
Corso d'Augusto 237, 47921 Rimini (Italy)

SPECIAL ISSUE This article is part of a Special Issue on Polypharmacology and Multitarget Drugs. To view the complete issue, visit: http://onlinelibrary.wiley.com/doi/10.1002/cmdc.v11.12/issuetoc.

cells, which leads to aberrant cell cycle progression[11] and to the accumulation of aging-associated abnormalities. p53 is an intrinsically unstable protein, the conformation and DNA binding domain of which can be modulated by metal chelators and redox status.[12] In particular, an alteration in oxidative homeostasis, resulting in sub-toxic and chronic exposure to reactive oxygen species (ROS), impairs the tertiary structure of wild-type p53, and this induces a switch toward the nonfunctional unfolded form of p53.[13] Alteration of the physiological functions of p53 can also result from exposure to soluble, nontoxic Aβ and has been shown to be related to the ability of Aβ to interfere with two key proteins, that is, zyxin and the homeodomain-interacting protein kinase 2 (HIPK2).[14] Zyxin is an adaptor protein identified as a regulator of HIPK2–p53 signaling in response to DNA damage.[15] The activity of HIPK2 is in turn fundamental in maintaining the function of wild-type p53, as it controls the destiny of cells upon exposure to DNA-damaging agents. In particular, soluble Aβ peptides downregulate zyxin expression, which is fundamental in maintaining the stability of HIPK2 and in turn the activity of p53.[14b] This Aβ-mediated downregulation may be responsible for early pathological changes that precede the amyloidogenic pathway in the neurodegenerative cascade. Therefore, the induction of the unfolded state of p53 by leading to the accumulation of dysfunctional neurons in the central nervous system, is emerging as a novel amyloid-based mechanism of AD pathogenesis.

As part of our ongoing work aimed at deepening our insight into the cross-talk between Aβ function and oxidative stress in AD, we envisioned nature as a structural "muse". Natural products offer great chemical diversity[16] and have already proven to be a rich source of therapeutics. Polyphenols are widely diffused in nature. They have been shown to modulate several AD pathways, including oxidative injuries and Aβ aggregation.[17] Interestingly, many of them present a hydroxycinnamoyl function as a recurring motif. On the other hand, diallyl sulfides are garlic-derived organosulfur compounds carrying allyl mercaptan moieties. They counteract oxidative stress through antioxidant enzyme expression.[18] Herein, we combined these privileged molecular fragments in new chemical entities to afford hybrids **1**–**3** (Figure 1).

The synthesized compounds were first tested in vitro to assess their anti-aggregating properties toward $A\beta_{42}$, the most amyloidogenic isoform of Aβ. They were then assayed in neuroblastoma cells to explore their ability to counteract oxidative stress and to exert a neuroprotective effect against $A\beta_{42}$-induced toxicity.

The efficacy of **1**–**3** in modulating an Aβ-induced conformational state alteration of the p53 protein was also investigated.

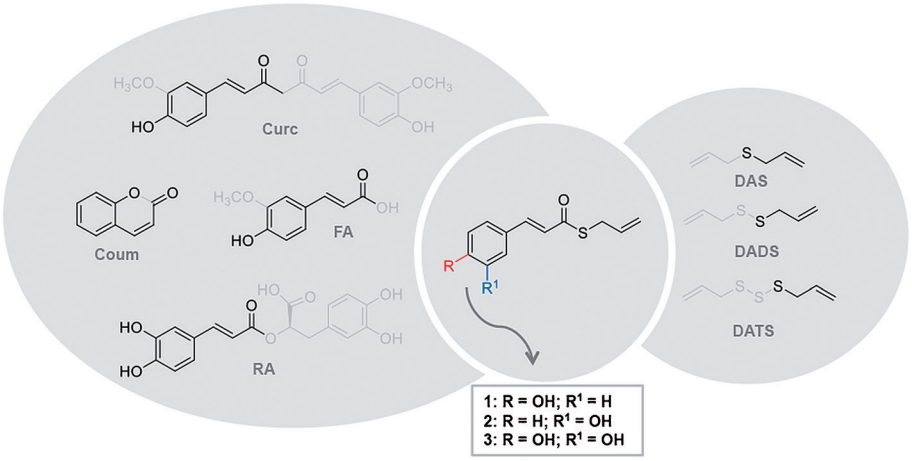

Figure 1. Design strategy for compounds **1**–**3**. Curc: curcumin, Coum: coumarin, FA: ferulic acid, RA: rosmarinic acid, DAS: diallyl sulfide, DADS: diallyl disulfide, DATS: diallyl trisulfide.

Curcumin was herein the reference compound. On the basis of its pleiotropic nature, curcumin is a consolidated prototype for AD studies, and it has already provided an outstanding platform for numerous biologically active ligands.[19]

Results and Discussion

Chemistry

The synthesis of **1**–**3** was performed in a linear fashion, as depicted in Scheme 1. *tert*-Butyldimethylsilyl (TBDMS) protection of the alcohol followed by coupling with *N*,*N*′-dicyclohexylcarbodiimide (DCC) in the presence of 4-(*N*,*N*-dimethylamino)pyridine (DMAP) gave intermediates **10**–**12**. Finally, treatment of **10**–**12** with tetrabutylammonium fluoride (TBAF) effected desilylation to give final compounds **1**–**3**.

The synthesized molecules were characterized by NMR spectroscopy and ESI mass spectrometry. The ^{1}H NMR spectra show that all compounds have the *E* configuration, as indicated by

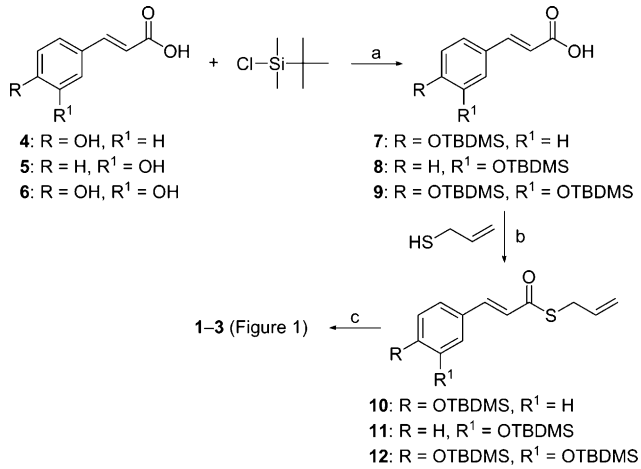

Scheme 1. *Reagents and conditions*: a) DMF, imidazole, N_2, overnight, RT; b) DCC, DMAP, CH_2Cl_2, N_2, overnight, 0 °C→RT; c) TBAF, THF, N_2, 30 min, RT.

the large coupling constants (~16 Hz) of the α-H and β-H protons on the double bonds.

Biological assays

Inhibition of Aβ$_{42}$ self-aggregation (thioflavin T-based assay)

We fostered the development of nature-inspired multifunctional ligands as an attractive opportunity to gain insight into the cross-talk between oxidative damage and Aβ pathways. Therefore, the synthesized compounds were first tested to evaluate their possible anti-aggregating properties by means of a thioflavin T (ThT)-based fluorimetric assay. ThT dye shows a characteristic redshift in the excitation/emission spectrum and an increase in the quantum yield upon binding to fibrillar β-sheet structures.[20] The ThT-based assay is commonly used to monitor Aβ fibrilization and its inhibition.

The evaluation of **1**–**3** clearly highlights a strong influence of the aryl decoration on the ability to prevent the Aβ$_{42}$ self-assembly process. Interestingly, the catechol moiety (compound **3**) turned out to be essential for activity. Compound **3**, in a 1:1 ratio with Aβ$_{42}$, almost completely inhibited the self-aggregation of Aβ$_{42}$ (inhibition > 90%), and it was even more effective than curcumin (inhibition = 73.7%). Notably, under the same experimental conditions, a complete loss of the anti-aggregating efficacy was observed for **1** and **2**, which lack the *m*- and *p*-hydroxy function, respectively (Figure 2).

This striking result points to the catechol moiety as a key recognition fragment in amyloid binding. The inhibitory effect exerted by **3** was found to be concentration dependent with an IC_{50} value of (12.5 ± 0.9) μM. On the basis of this value, **3** can be considered a good inhibitor of the self-aggregation of Aβ$_{42}$, as its inhibitory potency is similar to that of the well-known multipotent compound bis(7)tacrine [IC_{50} = (8.4 ± 1.4) μM][21] and similar to that of derivative D737 (IC_{50} ~ 10 μM);[22] furthermore, **3** is only fivefold less potent than the flavonoid myricetin [IC_{50} = (2.60 ± 0.33) μM].[23]

To explore the possibility of tuning the anti-aggregating profile of **3**, a detailed structure–activity relationship study is in progress, and the results will be published in due course.

Inhibition of Aβ$_{42}$ self-aggregation (mass spectrometry assay)

Motivated by the promising results, we sought to gain a deeper understanding of the mode of action of **3** at a molecular level by using an orthogonal method, that is, electrospray ionization ion trap mass spectrometry (ESI-IT-MS) in flow injection mode, which allows the monomeric form of Aβ$_{42}$ to be detected and quantitated.[23] Amyloid aggregation was monitored by evaluating the decrease in the amount of the Aβ monomer after 24 h incubation in the presence and absence of the tested inhibitor by using reserpine as the internal standard (IS). Under the experimental conditions, in the absence of any inhibitor a progressive decrease in the content of the monomer, expressed as the sum of the native (Aβ$_{42}$ Native) and oxidized forms (Aβ$_{42}$ Ox) of Aβ$_{42}$, was observed within 24 h owing to inclusion of the Aβ monomers into growing stable oligomers.[24] In agreement with this trend, upon incubating Aβ$_{42}$ alone, a dramatic decrease (83%) in the content of the monomer was observed after incubating for 24 h (Figure 3).

Conversely, upon treating Aβ$_{42}$ with **3** in a peptide/inhibitor ratio of 1:1, after incubating for 24 h a high monomer content was detected; consequently, **3** strongly inhibited inclusion of the monomer into growing amyloid oligomers (Figure 3). Indeed, the residual percentage of the Aβ$_{42}$ monomer at 24 h was only 17% in the absence of any inhibitor and 78% in the presence of **3**. Curcumin, tested under the same conditions, was a much weaker inhibitor of early-phase Aβ$_{42}$ aggregation (residual percentage of monomer after 24 h incubation: 36%).

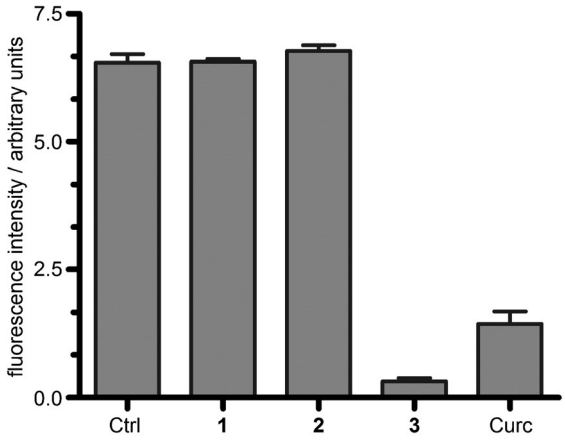

Figure 2. Inhibition of Aβ$_{42}$ aggregation by **1**–**3** or curcumin (Curc), as determined by a ThT-based assay. ThT-related fluorescence intensity of Aβ$_{42}$ (50 μM) samples after a 24 h incubation period in the absence (Ctrl) or in the presence of the indicated test compounds (all at 50 μM). Values are the mean ± SEM of two independent measurements each performed in duplicate.

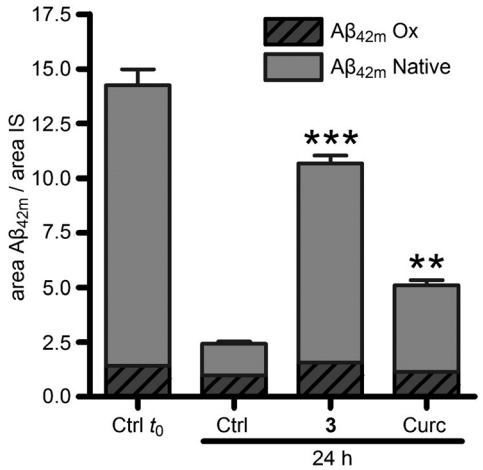

Figure 3. Inhibition of Aβ$_{42}$ aggregation by **3** and curcumin (Curc), both at 50 μM, as determined by ESI-IT-MS. The total Aβ$_{42}$ monomer (Aβ$_{42m}$) content in the absence (Ctrl) and in the presence of inhibitor is displayed as the sum of the native (Aβ$_{42}$ Native) and oxidized (Aβ$_{42}$ Ox) forms of Aβ$_{42}$. IS: internal standard (reserpine); $^{**}p < 0.01$, $^{***}p < 0.001$ versus Ctrl 24 h; Dunnett's multiple comparison test.

These results, other than confirming the anti-aggregating activity resulting from the ThT-based assay, also showed that **3** was able to strongly retard the overall assembly process of Aβ by acting at the monomer level in the early stage of amyloid aggregation and by strongly preventing the formation of stable soluble oligomers. This is of utmost importance because of the cytotoxic effects exerted by soluble aggregation intermediates.[25] The overall inhibition percentage was (74.5 ± 6.5) %, in agreement with the data obtained from the ThT fluorimetric assay. On the other hand, curcumin showed an inhibition of (22 ± 7.6) %.

Previous studies performed on the natural polyphenol myricetin showed pro-oxidant properties toward $A\beta_{42}$ peptide.[24] These properties can be explained by the well-accepted attitude of polyphenols to act as either antioxidant or pro-oxidant agents.[26] The oxidized form of $A\beta_{42}$ ($A\beta_{42}$ Ox) was shown to be less prone to aggregate than the native one ($A\beta_{42}$ Native), which thus explains the slower aggregation rate.[27] With these concepts in mind, we sought to verify whether **3**, bearing a catechol moiety, could partially exert its inhibitory activity through an oxidation-based mechanism. On the basis of their different molecular weights, both the native and oxidized forms of $A\beta_{42}$ can be detected by MS analysis. A small percentage of $A\beta_{42}$ Ox is always present in commercial samples of $A\beta_{42}$ (~15%, detectable at $t=0$), and in agreement with the lower inclination of $A\beta_{42}$ Ox to aggregate, the initial content of the oxidized Aβ species just slightly decreases after incubating for 24 h (Figure 3).[24]

Upon treating $A\beta_{42}$ samples with **3** in a peptide/inhibitor ratio of 1:1, only a slightly increase in the oxidized species after 24 h with respect to the initial content was observed, which thus excludes a significant oxidation-mediated mode of inhibition (Figure 3). Hence, on the basis of these results, stabilization of the $A\beta_{42}$ monomeric form and inhibition of its inclusion into growing oligomers, which greatly retards the overall assembly process of Aβ, can be postulated.

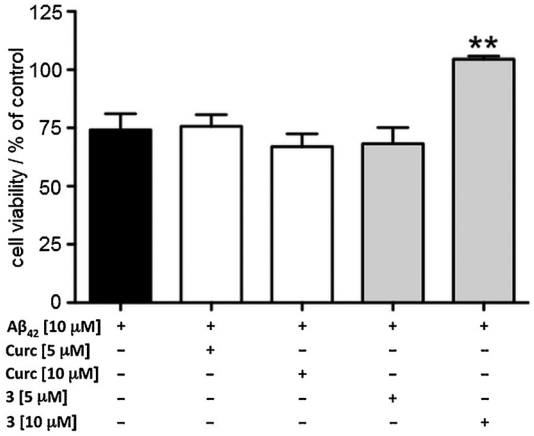

Figure 4. Effect of curcumin (Curc) and compound **3** on $A\beta_{42}$-mediated cytotoxicity in neuroblastoma cells. SH-SY5Y cells were pretreated for 24 h with curcumin or compound **3** at 5 or 10 μM and then incubated for an additional 24 h with $A\beta_{42}$ at 10 μM. Cell viability was determined by MTT assay. Data are expressed as percentage cell viability versus control; $^{**}p < 0.01$ versus $A\beta_{42}$; Dunnett's multiple comparison test.

Antioxidant effect on H_2O_2-induced damage

To determine the potential interest of thioesters **1**–**3** as antioxidants, we investigated their protective effects against H_2O_2-induced oxidative damage. The scavenging effect of ROS was evaluated in neuroblastoma cells by using the fluorescent probe dichlorofluorescein diacetate (DCF-DA) as a specific marker for the quantitative intracellular formation of ROS. In comparison with untreated neuroblastoma cells (dashed line, Figure 5), the intracellular DCF fluorescence intensity in H_2O_2-treated cells significantly increased (gray line, Figure 5). Treatment with curcumin and compounds **1**–**3** significantly suppressed the production of H_2O_2-induced intracellular ROS (Figure 5), and **2** was strongly more effective in counteracting the formation of ROS.

Protective effect of 3 on $A\beta_{42}$-induced toxicity in SH-SY5Y neuroblastoma cells

To determine whether **3** may exert any neuroprotective effect against $A\beta_{42}$-induced toxicity, a cell-viability study in SH-SY5Y human neuroblastoma cells was performed by using the 3-(4,5-dimethylthiazol-2-yl)-2,5-diphenyltetrazolium bromide (MTT) assay. Incubation of SH-SY5Y cells with 10 μM $A\beta_{42}$ resulted in a decrease in cell viability by approximately 25%, and this can be ascribed to the formation of oligomeric species.[28] Nontoxic concentrations of **3** and curcumin (5 and 10 μM) were then co-incubated with $A\beta_{42}$. The results depicted in Figure 4 clearly show that **3** is able to exert a dose-dependent protective effect. Indeed, whereas at a concentration of 5 μM of **3** could not prevent $A\beta_{42}$ cytotoxicity, a strong protective effect was observed if **3** was used at a concentration of 10 μM. At this concentration, **3** almost completely prevented Aβ-induced cell death. In the same assay, curcumin was not able to counteract Aβ toxicity even at a concentration of 10 μM.

Effect on the zyxin–HIPK2–p53 signaling pathway

The pro-oxidant environment induced by Aβ is well established in AD pathology, and a correlation among Aβ, oxidative stress, and conformational changes of p53 has already been suggested.[13,29]

In this context, our experimental setting was based on data from the literature indicating that sub-lethal concentrations of Aβ modulate oxidative stress by inducing high levels of oxidative markers, such as 4-hydroxy-2-nonenal Michael adducts and 3-nitrotyrosine, and by altering the conformation of p53 mainly as a result of nitration of its tyrosine residues.[30] However, it is notable that Aβ may also act as an antioxidant under specific conditions, and this ability seems to be dependent on the concentration of the peptide.[31]

The mechanisms by which Aβ induces the deregulation of zyxin and HIPK2 and consequent conformational changes in p53 may therefore be related to the capability of the peptide to alter oxidative homeostasis. If this is the case, compounds

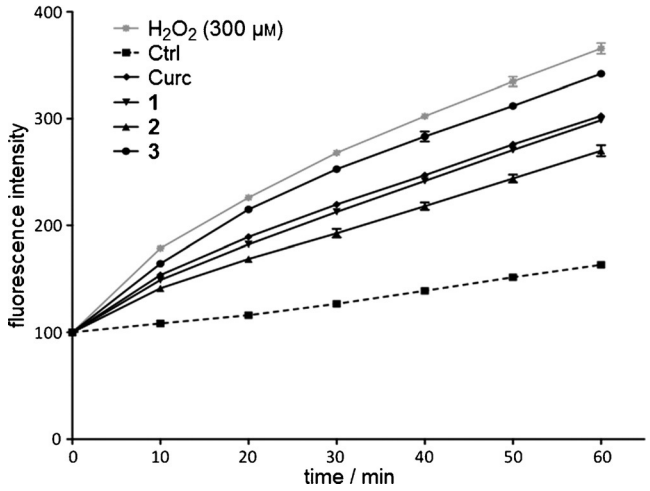

Figure 5. Compounds **1**–**3** reverse ROS-formation-induced oxidative stress. Cells were pretreated with curcumin (Curc) and compounds **1**–**3** (5 μM) for 24 h and then loaded with 25 μM DCF-DA for 45 min. DCF-DA was removed, and cells were then exposed to 300 μM H_2O_2. Intracellular ROS levels were determined on the basis of DCF fluorescence by using a fluorescent microplate. The graph shows the intracellular fluorescence intensity of DCF ± SD at various time treatments. Fluorescence intensity for curcumin and compounds **1**–**3** at any time is significant, with $p < 0.001$ versus H_2O_2; Dunnett's multiple comparison test.

with antioxidant activity should decrease conformational changes in p53 mediated by Aβ.

To substantiate this hypothesis, compounds **1**–**3** were further investigated in a neuroblastoma cell line to verify whether they may affect alterations in the zyxin–HIPK2–p53 pathway mediated by soluble sub-lethal concentrations of Aβ. For this experimental setting, we diluted Aβ in dimethyl sulfoxide, as evidence from the literature indicates that diluted solutions of Aβ peptides in this solvent are quite stable and are less prone to fibrilization at near-physiologic concentrations.[32]

We first characterized SH-SY5Y neuroblastoma cells in terms of HIPK2 and zyxin expression and the conformational status of p53. In agreement with our previous data,[14b] a sub-lethal concentration of $Aβ_{42}$ (10 nM) significantly decreased the protein levels of HIPK2 and zyxin (Figure 6a).

The conformational status of p53 was analyzed by immunoprecipitation by using two conformation-specific antibodies, that is, PAb1620 and PAb240, which discriminate between the folded and unfolded tertiary structures of p53, respectively.[33] As previously verified with other cell lines, in neuroblastoma cells $Aβ_{42}$ also induced the expression of unfolded p53, as recognized by the PAb240 antibody (Figure 6b).

On this basis, neuroblastoma cells were then treated with 10 nM $Aβ_{42}$ in the presence and absence of compounds **1**–**3** at

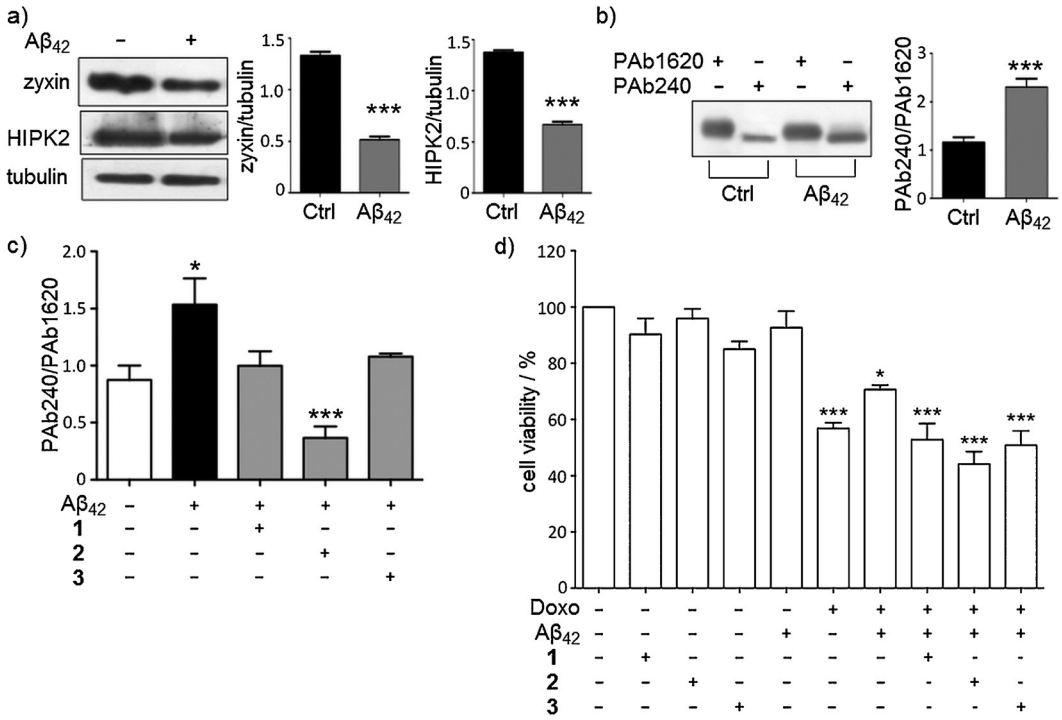

Figure 6. Compounds **1**–**3** positively modulate alterations in the zyxin–HIPK2–p53 pathway mediated by soluble sub-lethal levels of $Aβ_{42}$. a) Total cell extracts of SH-SY5Y cells treated with 10 nM $Aβ_{42}$ for 48 h were analyzed for zyxin and HIPK2 expression. Anti-tubulin was used as the protein loading control. b) SH-SY5Y cell lysates were immunoprecipitated with PAb240 or PAb1620 antibody. Immunoprecipitates were analyzed by western blot with the CM1 polyclonal anti-p53 antibody. c) Total cell extracts of SH-SY5Y cells incubated for 48 h with 10 nM $Aβ_{42}$ and then treated with 5 μM compounds **1**–**3** for 24 h were analyzed for the conformational state of p53. Cell lysates were immunoprecipitated with PAb240 or PAb1620 antibody. Immunoprecipitates were analyzed by western blot with the CM1 polyclonal anti-p53 antibody. After densitometric analysis, data were expressed as integrated density of the ratio of PAb240/PAb1620 antibodies signal and represent the mean ± SEM of at least three independent experiments; $*p < 0.05$, $***p < 0.001$ versus Aβ treatment; Tukey's multiple comparison test. d) SH-SY5Y cells were incubated with 10 nM $Aβ_{42}$ for 24 h and then treated for an additional 24 h with compounds **1**–**3** at 5 μM. Cells were then resuspended in fresh medium and finally exposed to 0.5 μM doxorubicin for 24 h. Cell viability was determined by MTT assay. Data are expressed as percentage cell viability versus control; $*p < 0.05$, $***p < 0.001$ versus control; Bonferroni multiple comparison test.

a concentration of 5 μM. Upon adding compounds **1**–**3** to the Aβ-pretreated cells, the level of unfolded p53 was significantly lowered, as the intensity of the PAb240-positive band was lower than that obtained for cells treated with $A\beta_{42}$ alone. The ratio between the intensities of the bands immunoreactive to PAb240 and PAb1620 was similar to that observed for the control cells (Figure 6c), for which **2** was significantly more effective. These data show that pretreatment of neuroblastoma cells, in particular with compound **2**, for which marked antioxidant properties are not accompanied by any anti-aggregating activity, prevented Aβ-induced conformational changes in p53. This finding may support the involvement of oxidative stress in Aβ function.

Loss of the wild-type conformation and function of p53 induced by soluble nontoxic Aβ has been shown to contribute to the accumulation of cell damage, which makes cells unable to activate the proper apoptotic program if exposed to noxae.[11a,14a,b] In light of this evidence, we sought to study cell sensitivity to doxorubicin, a genotoxic agent able to induce apoptosis in a p53-dependent manner,[34] following treatment with 10 nM $A\beta_{42}$ in the presence and absence of 5 μM **1**–**3**. Notably, cells treated with **1**–**3** and $A\beta_{42}$ were more vulnerable to doxorubicin than cells treated with $A\beta_{42}$ alone. Doxorubicin induced a decrease in cell viability by approximately 30% in Aβ-treated cells, whereas the decrease in cell viability was approximately 50% in the presence of $A\beta_{42}$ and each tested compound (Figure 6d). The obtained results indicate that compounds **1**–**3** may prevent the production of the unfolded isoform of p53 induced by Aβ, which makes the cells more sensitive and able to respond to an insult.

Conclusions

The amyloidogenic pathway is thought to be crucial to the complex nature of Alzheimer's disease. However, Aβ-centric drug programs have had limited success in AD clinical trials so far. Yet, growing evidence suggests that merely hitting Aβ production or aggregation will not be enough to undermine the architecture of AD, which calls for a deeper understanding of the functions of Aβ. To this aim, we synthesized three nature-inspired compounds to investigate the connection between Aβ and oxidative stress, and p53 emerged as a possible mediator of this functional interplay.

Interestingly, the hydroxy substituents on the aromatic moiety allowed strategic tuning of the pharmacological profiles of the compounds. Notably, of the three synthesized derivatives, only the catechol derivative (*S*)-allyl (*E*)-3-(3,4-dihydroxyphenyl)prop-2-enethioate inhibited the formation of Aβ fibrils, which underlines the importance of the catechol moiety. By acting at the early stage of amyloid aggregation, this catechol derivative strongly prevented the formation of cytotoxic stable oligomeric intermediates. Conversely, although to different extents, all hybrids were able to decrease the formation of ROS and to inhibit Aβ-induced conformational changes in p53, and the stronger antioxidant (*S*)-allyl (*E*)-3-(3-hydroxyphenyl)-prop-2-enethioate, which lacks anti-aggregating properties, was significantly more effective. These findings suggest the involvement of radical species in the loss of p53 conformation and function induced by sub-toxic levels of Aβ. Most importantly, the multifunctional ligand (*S*)-allyl (*E*)-3-(3,4-dihydroxyphenyl)prop-2-enethioate, together with compounds (*S*)-allyl (*E*)-3-(4-hydroxyphenyl)prop-2-enethioate and (*S*)-allyl (*E*)-3-(3-hydroxyphenyl)prop-2-enethioate, in which only the anti-aggregating activity was switched off, emerge as promising pharmacologic instruments that can be used to deepen our insight into the molecular mechanisms potentially involved in chronic Aβ injuries.

Experimental Section

Chemistry

General methods

Chemical reagents were purchased from Sigma–Aldrich, Fluka, and Lancaster (Italy). The reactions were monitored by thin-layer chromatography (TLC) on 0.20 mm silica gel 60 F_{254} plates (Merck, Germany), which were visualized with a UV lamp. NMR spectra were recorded at 400 MHz for ^{1}H and 100 MHz for ^{13}C with a Varian VXR 400 spectrometer. Chemical shifts are reported in parts per millions (ppm) relative to tetramethylsilane, and spin multiplicities are given as s (singlet), br s (broad singlet), d (doublet), t (triplet), q (quartet), and m (multiplet). Direct infusion ESI-MS mass spectra were recorded with a Waters ZQ 4000 apparatus. Final compounds **1**–**3** were >95% pure, as determined by HPLC analyses. The analyses were performed under reversed-phase conditions by using a Phenomenex Jupiter C18 (150×4.6 mm I.D.) column with the use of a binary mixture (A/B) of H_2O/CH_3CN (60:40 *v*/*v*) as the mobile phase, UV detection at $\lambda = 302$ nm, and a flow rate of 0.7 mL min^{-1}. Liquid chromatography was performed by using a Jasco Corporation (Tokyo, Japan) model PU-1585 UV equipped with a 20 μL loop valve.

Synthesis

General procedure for the synthesis of intermediates 7–9: TBDMSCl (2–3 equiv) and imidazole (5 equiv) were added to a solution of appropriate *trans*-cinnamic acid **4**–**6** (1 equiv) in dry DMF (5 mL) under a nitrogen atmosphere. The mixture was left at room temperature overnight, and then the mixture was concentrated to dryness and the residue was purified by column chromatography on silica gel to yield intermediate **7**–**9**. Compounds **4**–**6** are commercially available or can be synthesized as described in the literature for the synthesis of *trans*-cinnamic acid through the Knoevenagel–Doebner reaction.[35]

(*E*)-3-{4-[(*tert*-Butyldimethylsilyl)oxy]phenyl}acrylic acid (7): Synthesized from **4** (500 mg, 3.04 mmol). Elution with petroleum ether (PE)/EtOAc (6:4) afforded **7** as a waxy solid; yield: 466 mg (55%); ^{1}H NMR (400 MHz, $CDCl_3$): $\delta = 7.71$ (d, $J = 16.0$ Hz, 1H), 7.45 (d, $J = 8.0$ Hz, 2H), 6.85 (d, $J = 8.0$ Hz, 2H), 6.31 (d, $J = 16.0$ Hz, 1H), 0.99 (s, 9H), 0.23 ppm (s, 6H).

(*E*)-3-{3-[(*tert*-butyldimethylsilyl)oxy]phenyl}acrylic acid (8): Synthesized from **5** (500 mg, 3.04 mmol). Elution with PE/EtOAc (7:3) afforded **8** as a waxy solid; yield: 370 mg (44%); ^{1}H NMR (400 MHz, $CDCl_3$): $\delta = 7.72$ (d, $J = 16.0$ Hz, 1H), 7.24 (t, $J = 8.0$ Hz, 1H), 7.13 (d, $J = 8.0$ Hz, 1H), 7.00 (s, 1H), 6.87 (d, $J = 8.0$ Hz, 1H), 6.40 (d, $J = 16.0$ Hz, 1H), 0.98 (s, 9H), 0.20 ppm (s, 6H).

(*E*)-3-{3,4-Bis[(*tert*-butyldimethylsilyl)oxy]phenyl}acrylic acid (9): Synthesized from commercially available **6** (500 mg, 2.78 mmol). Elution with PE/EtOAc (8:2) afforded **9** as a waxy solid; yield: 318 mg (28%); ^{1}H NMR (400 MHz, $CDCl_3$): δ = 7.64 (d, J = 16.0 Hz, 1H), 7.02 (d, J = 8.0 Hz, 1H), 7.01 (s, 1H), 6.82 (d, J = 8.0 Hz, 1H), 6.22 (d, J = 16.0 Hz, 1H), 0.96 (s, 18H), 0.19 ppm (s, 12H).

General procedure for the synthesis of intermediates 10–12: DCC (1.1 equiv) and DMAP (cat.) were added to an ice-cooled solution of appropriate acid **7–9** (1 equiv) in dry CH_2Cl_2 (4 mL). The mixture was stirred for 10 min, which was followed by the addition of 2-propene-1-thiol (3 equiv). Stirring was continued at room temperature overnight; the mixture was filtered and concentrated. The crude material was purified by chromatography on silica gel.

(*S*)-Allyl (*E*)-3-{4-[(*tert*-butyldimethylsilyl)oxy]phenyl}prop-2-enethioate (10): Synthesized from **7** (160 mg, 0.575 mmol). Elution with PE/EtOAc (9.8:0.2) afforded **10** as a waxy solid; yield: 100 mg (52%); ^{1}H NMR (400 MHz, $CDCl_3$): δ = 7.57 (d, J = 15.6 Hz, 1H), 7.43 (d, J = 8.0 Hz, 2H), 6.84 (d, J = 8.0 Hz, 2H), 6.59 (d, J = 15.6 Hz, 1H), 5.88–5.83 (m, 1H), 5.28 (d, J = 17.0 Hz, 1H), 5.13 (d, J = 10.0 Hz, 1H), 3.66 (d, J = 6.8, 2H), 0.98 (s, 9H), 0.22 ppm (s, 6H).

(*S*)-Allyl (*E*)-3-{3-[(*tert*-butyldimethylsilyl)oxy]phenyl}prop-2-enethioate (11): Synthesized from **8** (370 mg, 1.33 mmol). Elution with PE/EtOAc (9.8:0.2) afforded **11** as a waxy solid; yield: 260 mg (58%); ^{1}H NMR (400 MHz, $CDCl_3$): δ = 7.57 (d, J = 15.6 Hz, 1H), 7.15 (t, J = 8 Hz, 1H), 7.13 (s, 1H), 6.88 (d, J = 8.0 Hz, 1H), 6.70 (d, J = 8.0 Hz, 1H), 6.66 (d, J = 16.0 Hz, 1H), 5.88–5.83 (m, 1H), 5.28 (d, J = 16.0 Hz, 1H), 5.13 (d, J = 10.0 Hz 1H), 3.66 (d, J = 6.4 Hz, 2H), 0.97 (s, 9H), 0.20 ppm (s, 6H).

(*S*)-Allyl (*E*)-3-{3,4-bis[(*tert*-butyldimethylsilyl)oxy]phenyl}prop-2-enethioate (12): Synthesized from **9** (200 mg, 0.500 mmol). Elution with PE/EtOAc (9.5:0.5) afforded **12** as a waxy solid; yield: 160 mg (70%); ^{1}H NMR (400 MHz, $CDCl_3$): δ = 7.49 (d, J = 16 Hz, 1H), 7.00 (d, J = 8.0 Hz, 1H), 6.80 (d, J = 8.0 Hz, 1H), 6.72 (s, 1H), 6.50 (d, J = 16.0 Hz, 1H), 5.76–5.65 (m, 1H), 5.25 (d, J = 16.8 Hz, 1H), 5.09 (d, J = 10.1 Hz, 1H), 3.56 (d, J = 6.8 Hz, 2H), 0.97 (s, 9H), 0.96 (s, 9H), 0.19 (s, 6H), 0.18 ppm (s, 6H).

General procedure for the synthesis of 1–3: TBAF (4 equiv) was added to a solution of appropriate organosilane intermediate **10–12** (1 equiv) in THF (5 mL) and stirring was continued at room temperature. After 20–30 min, the reaction was quenched by the addition of a saturated aqueous NH_4Cl solution; the aqueous phase was extracted with EtOAc (3×10 mL), and the combined organic layer was dried (Na_2SO_4). Following evaporation of the solvent, the residue was purified by column chromatography on silica gel.

(*S*)-Allyl (*E*)-3-(4-hydroxyphenyl)prop-2-enethioate (1): Synthesized from **10** (100 mg, 0.299 mmol). Elution with PE/EtOAc (7:3) afforded **1** as a waxy solid; yield: 30 mg (46%); ^{1}H NMR (400 MHz, $CDCl_3$): δ = 7.56 (d, J = 16.0 Hz, 1H), 7.42 (d, J = 8.0 Hz, 2H), 6.84 (d, J = 8.0 Hz, 2H), 6.58 (d, J = 16.0 Hz, 1H), 5.88–5.81 (m, 1H), 5.29–5.25 (d, J = 17.0 Hz, 1H), 5.13–5.10 (d, J = 10.0 Hz, 1H), 3.65 ppm (d, J = 8.0 Hz, 2H); ^{13}C NMR (100 MHz, $CDCl_3$): δ = 189.97, 158.23, 140.83, 133.05, 130.44, 126.66, 122.29, 118.02, 116.03, 31.80 ppm; MS (ESI+): m/z: 243 $[M+Na]^+$.

(*S*)-Allyl (*E*)-3-(3-hydroxyphenyl)prop-2-enethioate (2): Synthesized from **11** (210 mg, 0.63 mmol). Elution with CH_2Cl_2/MeOH (9.7:0.3) afforded **2** as a waxy solid; yield: 110 mg (79%); ^{1}H NMR (400 MHz, $CDCl_3$): δ = 7.54 (d, J = 16.0 Hz, 1H), 7.24 (t, J = 8.0 Hz, 1H), 7.08 (d, J = 8.0 Hz, 1H), 7.02 (s, 1H), 6.90 (d, J = 8.0 Hz, 1H), 6.58 (d, J = 16.0 Hz, 1H), 6.09 (br s, 1H), 5.88–5.81 (m, 1H), 5.28 (d, J = 16.0 Hz, 1H), 5.13 (d, J = 10 Hz, 1H), 3.65 ppm (d, J = 6.4 Hz, 2H); ^{13}C NMR (100 MHz,$CDCl_3$): δ = 190.33, 156.20, 140.85, 135.43, 132.75, 130.22, 124.89, 121.12, 118.31, 118.05, 114.91, 31.94 ppm; MS (ESI−): m/z: 219 $[M-H]^-$.

(*S*)-Allyl (*E*)-3-(3,4-dihydroxyphenyl)prop-2-enethioate (3): Synthesized from **12** (160 mg, 0.344 mmol). Elution with PE/EtOAc (5:5) afforded **3** as a waxy solid; yield: 50 mg (62%); ^{1}H NMR (400 MHz, CD_3OD): δ = 7.54 (d, J = 16.0 Hz, 1H), 7.10 (s, 1H), 7.02 (d, J = 8.0 Hz, 1H), 6.84 (d, J = 8.0 Hz, 1H), 6.63 (d, J = 16.0 Hz, 1H), 5.94–5.87 (m, 1H), 5.31 (d, J = 16.8 Hz, 1H), 5.14 (d, J = 10.1 Hz, 1H), 3.68 ppm (d, J = 6.4 Hz, 2H); ^{13}C NMR (100 MHz, CD_3OD): δ = 189.34, 148.56, 145.47, 141.37, 133.43, 125.91, 122.14, 120.93, 116.56, 115.18, 113.93, 30.94 ppm; MS (ESI+): m/z: 259 $[M+Na]^+$.

Biological methods

Sample preparation for $A\beta_{42}$ self-aggregation: 1,1,1,3,3,3-Hexafluoro-2-propanol (HFIP)-pretreated $A\beta_{42}$ samples (Bachem AG, Switzerland) were resolubilized with a CH_3CN/0.3 mM Na_2CO_3/250 mM NaOH (48.4:48.4:3.2) mixture to have a stable stock solution ($[A\beta_{42}]$ = 500 μM).[36] Tested inhibitors were dissolved in MeOH and diluted in the assay buffer. Experiments were performed by incubating the peptide diluted in 10 mM phosphate buffer (pH 8.0) containing 10 mM NaCl at 30 °C (Thermomixer Comfort, Eppendorf, Italy) for 24 h (final Aβ concentration = 50 μM) with and without inhibitor.

Inhibition of $A\beta_{42}$ self-aggregation as determined by the ThT assay: Inhibition studies were performed by incubating $A\beta_{42}$ samples under the assay conditions reported above, with and without tested inhibitors. Inhibitors were first screened at 50 μM in a 1:1 ratio with $A\beta_{42}$. To quantify amyloid fibril formation, the ThT fluorescence method was used.[20b,37] After incubation, samples were diluted to a final volume of 2.0 mL with 50 mM glycine–NaOH buffer (pH 8.5) containing 1.5 μM ThT. A 300 s time scan of fluorescence intensity was performed (λ_{exc} = 446 nm; λ_{em} = 490 nm), and values at plateau were averaged after subtracting the background fluorescence of 1.5 μM ThT solution. Blanks containing inhibitor and ThT were also prepared and evaluated to account for quenching and fluorescence properties. The fluorescence intensities were compared and the percentage inhibition was calculated. For compound **3**, the IC_{50} value was also determined. To this aim, four increasing concentrations were tested. The IC_{50} value was obtained from the plot of percentage inhibition versus log(concentration of inhibitor).

*Inhibition of $A\beta_{42}$ self-aggregation by **3**, as determined by flow injection ESI-MS*: Inhibition studies were performed by incubating $A\beta_{42}$ samples under the assay conditions reported above, with and without tested inhibitor **3** or curcumin. At t = 0 and t = 24 h, aliquots with and without inhibitor were analyzed by flow injection (FIA) ESI-IT-MS. FIA–MS analyses were performed, as described by Fiori et al.[24] Briefly, the $A\beta_{42}$ samples were analyzed by 10 μL loop injection after previous addition of reserpine as internal standard. ESI-IT-MS analyses were performed with a Jasco PU-1585 Liquid Chromatograph (Jasco, Tokyo, Japan) interfaced with a LCQ Duo Mass Spectrometer (Thermo Finnigan, San Jose, CA, USA) equipped with an ESI source and operating with an ion-trap analyzer. The mobile phase consisted of 0.1% (*v*/*v*) formic acid in CH_3CN/H_2O (30:70). The ESI system employed a 4.5 kV spray voltage and a capillary temperature of 200 °C. Mass spectra were operated in positive polarity, in the scan range of m/z = 200 to 2000 at the scan rate of three microscans per second. Single-ion monitoring (SIM) chromatograms for the quantitative analysis were reconstructed at the base peaks corresponding to the differently charged amyloid mo-

nomer ions (Native, N) and oxidized ions (Ox). The ratio between the total monomer area and the IS area was used for $A\beta_{42}$ monomer determination. The $area_{total\ monomer}/area_{IS}$ ratio at $t=0$ was considered 100% of the monomer content. The results are expressed as mean ± SD of three independent experiments, and $p<0.05$ was considered statistically significant (Dunnett's multiple comparison test).

Reagents for cellular experiments: All culture media, supplements and fetal bovine serum (FBS) were obtained from Euroclone (Life Science Division, Milan, Italy). Electrophoresis reagents were obtained from Bio-Rad (Hercules, CA, USA). All other reagents were of the highest grade available and were purchased from Sigma Chemical Co. (St. Louis, MO, USA) unless otherwise indicated. $A\beta_{42}$ was solubilized in DMSO at a concentration of 100 μM and frozen in stock aliquots that were diluted at the final concentration of 10 nM prior to use. For each experimental setting, one aliquot of the stock was thawed out and diluted at the final concentration of 10 nM to minimize peptide damage as a result of repeated freeze and thaw. The $A\beta_{42}$ concentration was chosen following dose–response experiments (data not shown), for which maximal modulation of the p53 structure and its transcriptional activity[38] were obtained at 10 nM. All of the experiments performed with $A\beta_{42}$ were made in 1% serum. H_2O_2 was diluted to working concentration (1 mM) in phosphate-buffered saline (PBS) at the moment of use. Mouse monoclonal anti α-tubulin was purchased from Sigma–Aldrich (St. Louis, MO, USA). Host-specific peroxidase conjugated IgG secondary antibodies were obtained from Pierce (Rockford, IL, USA).

Cell cultures: Human neuroblastoma SH-SY5Y cells from European Collection of Cell Cultures (ECACC No. 94030304) were cultured in medium with equal amount of Eagle's minimum essential medium and Nutrient Mixture Ham's F-12, supplemented with 10% FBS, glutamine (2 mM), penicillin/streptomycin, nonessential amino acids at 37 °C in 5% CO_2/95% air.

Cell viability: The mitochondrial dehydrogenase activity that reduces 3-(4,5-dimethylthiazol-2-yl)-2,5-diphenyltetrazolium bromide (MTT; Sigma, St. Louis, MO, USA) was used to determine cellular viability, in a quantitative colorimetric assay. At day 0, SH-SY5Y cells were plated at a density of 2×10^4 viable cells per well in 96-well plates. After treatment, according to the experimental setting, cells were exposed to MTT solution in PBS (1 mg mL^{-1}). Following 4 h incubation with MTT and treatment with sodium dodecyl sulfate (SDS) for 24 h, cell viability reduction was quantified by using a BIO-RAD microplate reader (Model 550; Hercules, CA, USA).

Measurement of intracellular ROS: 2′,7′-Dichlorofluorescin diacetate (DCF-DA; Sigma–Aldrich) was used to estimate intracellular ROS. Briefly, cells (2×10^4 cells per well) were pretreated with reference curcumin and compounds **1**–**3** (5 μM) for 24 h and then loaded with 25 μM DCF-DA at 37 °C for 45 min. DCF-DA was removed after centrifuge and cells were resuspended in PBS and then exposed to 300 μM H_2O_2. The results were visualized by using a Synergy HT microplate reader (BioTek) with excitation and emission wavelengths of 485 and 530 nm, respectively.

Immunodetection of zyxin and HIPK2: Cell monolayers were washed with ice-cold PBS (2×5 mL), lysed on the tissue culture dish by addition of ice-cold lysis buffer [50 mM Tris·HCl pH 7.4, 150 mM NaCl, 50 mM EDTA, 0.2 mM 4-(2-aminoethyl)benzenesulfonylfluoride hydrochloride (AEBSF), 20 μg mL^{-1} leupeptin, 25 μg mL^{-1} aprotinin, 0,5 μg mL^{-1} pepstatin A, and 1% Triton X-100], and an aliquot was used for protein analysis with the Pierce Bicinchoninic Acid kit, for protein quantification. Cell lysates were diluted in sample buffer (62.5 mM Tris·HCl pH 6.8, 2% SDS, 10% glycerol, 50 mM dithiothreitol, 0.1% bromophenol blue) and subjected to western blot analysis. Proteins were subjected to SDS-PAGE (8%) and then transferred onto a polyvinylidene fluoride (PVDF) membrane 0.45 μm (Immobilion, Millipore Corp, Bedford, MA, USA). The membrane was blocked for 1 h with 5% nonfat dry milk in Tris-buffered saline containing 0.1% Tween 20 (TBST). Membranes were immunoblotted with the rabbit antihuman zyxin or HIPK2 polyclonal antibody (at 1:1000 dilution in 5% nonfat dry milk, from Cell Signaling Technology, EuroClone, Milan, Italy). Detection was performed by incubation with horseradish peroxidase conjugated goat anti-rabbit IgG (1:5000 dilution in 5% nonfat dry milk, from Pierce, Rockford, IL, USA) for 1 h. The blots were then washed extensively and the proteins of interest were visualized by using an enhanced chemiluminescent method (Pierce, Rockford, IL, USA). Tubulin was also performed as a normal control of proteins.

p53 conformational immunoprecipitation: The conformational state of p53 was analyzed by immunoprecipitation as detailed previously.[10a] Briefly, cells were lysed in immunoprecipitation buffer (10 mM Tris, pH 7.6, 140 mM NaCl, and 0.5% NP40 including protease inhibitors); 100 μg of total cell extracts was used for immunoprecipitation experiments performed in a volume of 500 μL with 1 μg of the conformation-specific antibodies PAb1620 (wild-type specific) or PAb240 (mutant specific; Neomarkers, CA, USA). Immunocomplexes were separated by 10% SDS-PAGE and immunoblotting was performed with rabbit anti-p53 antibody (FL393; Santa Cruz, CA, USA). Immunoreactivity was detected with the ECL-chemiluminescence reaction kit (Amersham, Little Chalfont, UK).

Densitometry and statistics

All experiments, unless specified, were performed at least three times. Following acquisition of the western blot image through an AGFA scanner and analysis by means of the Image 1.47 program (Wayne Rasband, NIH, Research Services Branch, NIMH, Bethesda, MD, USA), the relative densities of the bands were analyzed as described previously.[39] The data were analyzed by analysis of variance (ANOVA) followed, if significant, by an appropriate post hoc comparison test, as indicated in the figure legends. The reported data are expressed as mean ± SD of at least three independent experiments. Values $p<0.05$ were considered statistically significant.

Acknowledgements

The authors thank the University of Bologna (grants from the RFO), the University of Pavia (grants from the FAR–Fondo Ateneo Ricerca), and Unirimini for financial support.

Keywords: Alzheimer's disease · antioxidants · amyloid-beta peptide · p53 · multifunctional ligands

[1] a) D. J. Selkoe, *Behav. Brain Res.* **2008**, *192*, 106–113; b) J. Laurén, D. A. Gimbel, H. B. Nygaard, J. W. Gilbert, S. M. Strittmatter, *Nature* **2009**, *457*, 1128–1132.

[2] a) E. Karran, M. Mercken, B. De Strooper, *Nat. Rev. Drug Discovery* **2011**, *10*, 698–712; b) K. Herrup, *Nat. Neurosci.* **2015**, *18*, 794–799.

[3] a) E. Mura, F. Pistoia, M. Sara, S. Sacco, A. Carolei, S. Govoni, *Curr. Pharm. Des.* **2014**, *20*, 4121–4139; b) L. M. Ittner, J. Götz, *Nat. Rev. Neurosci.* **2011**, *12*, 65–72; c) Z. Esposito, L. Belli, S. Toniolo, G. Sancesario, C. Bianconi, A. Martorana, *CNS Neurosci. Ther.* **2013**, *19*, 549–555.

[4] a) E. Viayna, I. Sola, M. Bartolini, A. De Simone, C. Tapia-Rojas, F. G. Serrano, R. Sabaté, J. Juárez-Jiménez, B. Pérez, F. J. Luque, V. Andrisano, M. V.

Clos, N. C. Inestrosa, D. Muñoz-Torrero, *J. Med. Chem.* **2014**, *57*, 2549 – 2567; b) E. Nepovimova, E. Uliassi, J. Korabecny, L. E. Peña-Altamira, S. Samez, A. Pesaresi, G. E. Garcia, M. Bartolini, V. Andrisano, C. Bergamini, R. Fato, D. Lamba, M. Roberti, K. Kuca, B. Monti, M. L. Bolognesi, *J. Med. Chem.* **2014**, *57*, 8576 – 8589; c) M. Rosini, E. Simoni, M. Bartolini, E. Soriano, J. Marco-Contelles, V. Andrisano, B. Monti, M. Windisch, B. Hutter-Paier, D. W. McClymont, I. R. Mellor, M. L. Bolognesi, *ChemMedChem* **2013**, *8*, 1276 – 1281; d) M. Rosini, V. Andrisano, M. Bartolini, M. L. Bolognesi, P. Hrelia, A. Minarini, A. Tarozzi, C. Melchiorre, *J. Med. Chem.* **2005**, *48*, 360 – 363; e) M. Rosini, E. Simoni, M. Bartolini, A. Cavalli, L. Ceccarini, N. Pascu, D. W. McClymont, A. Tarozzi, M. L. Bolognesi, A. Minarini, V. Tumiatti, V. Andrisano, I. R. Mellor, C. Melchiorre, *J. Med. Chem.* **2008**, *51*, 4381 – 4384.

[5] a) A. Cavalli, M. L. Bolognesi, A. Minarini, M. Rosini, V. Tumiatti, M. Recanatini, C. Melchiorre, *J. Med. Chem.* **2008**, *51*, 347 – 372; b) M. Rosini, *Future Med. Chem.* **2014**, *6*, 485 – 487; c) A. Anighoro, J. Bajorath, G. Rastelli, *J. Med. Chem.* **2014**, *57*, 7874 – 7887.

[6] M. Rosini, E. Simoni, A. Milelli, A. Minarini, C. Melchiorre, *J. Med. Chem.* **2014**, *57*, 2821 – 2831.

[7] M. Coma, F. X. Guix, G. Ill-Raga, I. Uribesalgo, F. Alameda, M. A. Valverde, F. J. Muñoz, *Neurobiol. Aging* **2008**, *29*, 969 – 980.

[8] A. M. Swomley, S. Förster, J. T. Keeney, J. Triplett, Z. Zhang, R. Sultana, D. A. Butterfield, *Biochim. Biophys. Acta, Gen. Subj.* **2014**, *1842*, 1248 – 1257.

[9] a) S. Salvioli, M. Capri, L. Bucci, C. Lanni, M. Racchi, D. Uberti, M. Memo, D. Mari, S. Govoni, C. Franceschi, *Cancer Immunol. Immunother.* **2009**, *58*, 1909 – 1917; b) W. Chatoo, M. Abdouh, G. Bernier, *Antioxid. Redox Signaling* **2011**, *15*, 1729 – 1737; c) A. Salminen, K. Kaarniranta, *Cell. Signalling* **2011**, *23*, 747 – 752.

[10] a) D. Uberti, C. Lanni, T. Carsana, S. Francisconi, C. Missale, M. Racchi, S. Govoni, M. Memo, *Neurobiol. Aging* **2006**, *27*, 1193 – 1201; b) C. Lanni, M. Racchi, G. Mazzini, A. Ranzenigo, R. Polotti, E. Sinforiani, L. Olivari, M. Barcikowska, M. Styczynska, J. Kuznicki, A. Szybinska, S. Govoni, M. Memo, D. Uberti, *Mol. Psychiatry* **2008**, *13*, 641 – 647; c) X. Zhou, J. Jia, *Neurosci. Lett.* **2010**, *468*, 320 – 325.

[11] a) D. Uberti, T. Carsana, E. Bernardi, L. Rodella, P. Grigolato, C. Lanni, M. Racchi, S. Govoni, M. Memo, *J. Cell Sci.* **2002**, *115*, 3131 – 3138; b) Y. Yang, D. S. Geldmacher, K. Herrup, *J. Neurosci.* **2001**, *21*, 2661 – 2668.

[12] P. Hainaut, J. Milner, *Cancer Res.* **1993**, *53*, 4469 – 4473.

[13] C. Lanni, M. Racchi, M. Memo, S. Govoni, D. Uberti, *Free Radical Biol. Med.* **2012**, *52*, 1727 – 1733.

[14] a) C. Lanni, L. Nardinocchi, R. Puca, S. Stanga, D. Uberti, M. Memo, S. Govoni, G. D'Orazi, M. Racchi, *PLoS One* **2010**, *5*, e10171; b) C. Lanni, D. Necchi, A. Pinto, E. Buoso, L. Buizza, M. Memo, D. Uberti, S. Govoni, M. Racchi, *J. Neurochem.* **2013**, *125*, 790 – 799; c) E. Mura, S. Zappettini, S. Preda, F. Biundo, C. Lanni, M. Grilli, A. Cavallero, G. Olivero, A. Salamone, S. Govoni, M. Marchi, *PLoS One* **2012**, *7*, e29661.

[15] J. Crone, C. Glas, K. Schultheiss, J. Moehlenbrink, E. Krieghoff-Henning, T. G. Hofmann, *Cancer Res.* **2011**, *71*, 2350 – 2359.

[16] S. Rizzo, H. Waldmann, *Chem. Rev.* **2014**, *114*, 4621 – 4639.

[17] a) C. B. Pocernich, M. L. Lange, R. Sultana, D. A. Butterfield, *Curr. Alzheimer Res.* **2011**, *8*, 452 – 469; b) M. Stefani, S. Rigacci, *Int. J. Mol. Sci.* **2013**, *14*, 12411 – 12457.

[18] S. Kim, H. G. Lee, S. A. Park, J. K. Kundu, Y. S. Keum, Y. N. Cha, H. K. Na, Y. J. Surh, *PLoS One* **2014**, *9*, e85984.

[19] a) G. Gerenu, K. Liu, J. E. Chojnacki, J. M. Saathoff, P. Martinez-Martin, G. Perry, X. Zhu, H. G. Lee, S. Zhang, *ACS Chem. Neurosci.* **2015**, *6*, 1393 – 1399; b) E. Simoni, C. Bergamini, R. Fato, A. Tarozzi, S. Bains, R. Motterlini, A. Cavalli, M. L. Bolognesi, A. Minarini, P. Hrelia, G. Lenaz, M. Rosini, C. Melchiorre, *J. Med. Chem.* **2010**, *53*, 7264 – 7268.

[20] a) M. Groenning, L. Olsen, M. van de Weert, J. M. Flink, S. Frokjaer, F. S. Jørgensen, *J. Struct. Biol.* **2007**, *158*, 358 – 369; b) H. Naiki, K. Higuchi, M. Hosokawa, T. Takeda, *Anal. Biochem.* **1989**, *177*, 244 – 249.

[21] A. Minarini, A. Milelli, V. Tumiatti, M. Rosini, E. Simoni, M. L. Bolognesi, V. Andrisano, M. Bartolini, E. Motori, C. Angeloni, S. Hrelia, *Neuropharmacology* **2012**, *62*, 997 – 1003.

[22] A. F. McKoy, J. Chen, T. Schupbach, M. H. Hecht, *J. Biol. Chem.* **2012**, *287*, 38992 – 39000.

[23] M. Bartolini, M. Naldi, J. Fiori, F. Valle, F. Biscarini, D. V. Nicolau, V. Andrisano, *Anal. Biochem.* **2011**, *414*, 215 – 225.

[24] J. Fiori, M. Naldi, M. Bartolini, V. Andrisano, *Electrophoresis* **2012**, *33*, 3380 – 3386.

[25] a) C. G. Glabe, R. Kayed, *Neurology* **2006**, *66*, S74 – 78; b) M. P. Lambert, A. K. Barlow, B. A. Chromy, C. Edwards, R. Freed, M. Liosatos, T. E. Morgan, I. Rozovsky, B. Trommer, K. L. Viola, P. Wals, C. Zhang, C. E. Finch, G. A. Krafft, W. L. Klein, *Proc. Natl. Acad. Sci. USA* **1998**, *95*, 6448 – 6453; c) D. M. Walsh, I. Klyubin, J. V. Fadeeva, W. K. Cullen, R. Anwyl, M. S. Wolfe, M. J. Rowan, D. J. Selkoe, *Nature* **2002**, *416*, 535 – 539.

[26] S. C. Forester, J. D. Lambert, *Mol. Nutr. Food Res.* **2011**, *55*, 844 – 854.

[27] L. Hou, I. Kang, R. E. Marchant, M. G. Zagorski, *J. Biol. Chem.* **2002**, *277*, 40173 – 40176.

[28] S. Sabella, M. Quaglia, C. Lanni, M. Racchi, S. Govoni, G. Caccialanza, A. Calligaro, V. Bellotti, E. De Lorenzi, *Electrophoresis* **2004**, *25*, 3186 – 3194.

[29] L. R. Borza, *Rev. Med.-Chir. Soc. Med. Nat. Iasi* **2014**, *118*, 19 – 27.

[30] a) L. Buizza, C. Prandelli, S. A. Bonini, A. Delbarba, G. Cenini, C. Lanni, E. Buoso, M. Racchi, S. Govoni, M. Memo, D. Uberti, *Cell Death Dis.* **2013**, *4*, e484; b) L. Buizza, G. Cenini, C. Lanni, G. Ferrari-Toninelli, C. Prandelli, S. Govoni, E. Buoso, M. Racchi, M. Barcikowska, M. Styczynska, A. Szybinska, D. A. Butterfield, M. Memo, D. Uberti, *PLoS One* **2012**, *7*, e29789; c) G. Cenini, G. Maccarinelli, C. Lanni, S. A. Bonini, G. Ferrari-Toninelli, S. Govoni, M. Racchi, D. A. Butterfield, M. Memo, D. Uberti, *Amino Acids* **2010**, *39*, 271 – 283.

[31] D. G. Smith, R. Cappai, K. J. Barnham, *Biochim. Biophys. Acta* **2007**, *1768*, 1976 – 1990.

[32] H. Levine III, *Anal. Biochem.* **2004**, *335*, 81 – 90.

[33] C. Méplan, M. J. Richard, P. Hainaut, *Biochem. Pharmacol.* **2000**, *59*, 25 – 33.

[34] a) K. Hayakawa, M. Hasegawa, M. Kawashima, Y. Nakamura, M. Matsuura, H. Toda, N. Mitsuhashi, H. Niibe, *Oncol. Rep.* **2000**, *7*, 267 – 270; b) E. Lorenzo, C. Ruiz-Ruiz, A. J. Quesada, G. Hernández, A. Rodríguez, A. López-Rivas, J. M. Redondo, *J Biol. Chem.* **2002**, *277*, 10883 – 10892; c) S. Wang, E. A. Konorev, S. Kotamraju, J. Joseph, S. Kalivendi, B. Kalyanaraman, *J. Biol. Chem.* **2004**, *279*, 25535 – 25543.

[35] C. N. Xia, H. B. Li, F. Liu, W. X. Hu, *Bioorg. Med. Chem. Lett.* **2008**, *18*, 6553 – 6557.

[36] M. Bartolini, C. Bertucci, M. L. Bolognesi, A. Cavalli, C. Melchiorre, V. Andrisano, *ChemBioChem* **2007**, *8*, 2152 – 2161.

[37] H. Levine III, *Protein Sci.* **1993**, *2*, 404 – 410.

[38] D. Uberti, G. Cenini, L. Olivari, G. Ferrari-Toninelli, E. Porrello, C. Cecchi, A. Pensalfini, A. Pensafini, G. Liguri, S. Govoni, M. Racchi, M. Maurizio, *J. Neurochem.* **2007**, *103*, 322 – 333.

[39] C. Lanni, M. Mazzucchelli, E. Porrello, S. Govoni, M. Racchi, *Eur. J. Biochem.* **2004**, *271*, 3068 – 3075.

Received: September 15, 2015
Published online on October 26, 2015